

# A new malaria vector in Africa: Predicting the expansion range of *Anopheles stephensi* and identifying the urban populations at risk

M. E. Sinka<sup>a,1</sup> , S. Pironon<sup>b</sup> , N. C. Massey<sup>c</sup>, J. Longbottom<sup>d</sup> , J. Hemingway<sup>d,1</sup> , C. L. Moyes<sup>c,2</sup> , and K. J. Willis<sup>a,b,2</sup>

<sup>a</sup>Department of Zoology, University of Oxford, Oxford, United Kingdom, OX1 3SZ; <sup>b</sup>Biodiversity Informatics and Spatial Analysis Department, Royal Botanic Gardens Kew, Richmond, Surrey, United Kingdom, TW9 3DS; <sup>c</sup>Big Data Institute, Li Ka Shing Centre for Health Information and Discovery, University of Oxford, Oxford, United Kingdom, OX3 7LF; and <sup>d</sup>Department of Vector Biology, Liverpool School of Tropical Medicine, Liverpool, United Kingdom, L3 5QA

Edited by Nils Chr. Stenseth, University of Oslo, Norway, and approved July 27, 2020 (received for review March 26, 2020)

In 2012, an unusual outbreak of urban malaria was reported from Djibouti City in the Horn of Africa and increasingly severe outbreaks have been reported annually ever since. Subsequent investigations discovered the presence of an Asian mosquito species; *Anopheles stephensi*, a species known to thrive in urban environments. Since that first report, *An. stephensi* has been identified in Ethiopia and Sudan, and this worrying development has prompted the World Health Organization (WHO) to publish a vector alert calling for active mosquito surveillance in the region. Using an up-to-date database of published locational records for *An. stephensi* across its full range (Asia, Arabian Peninsula, Horn of Africa) and a set of spatial models that identify the environmental conditions that characterize a species' preferred habitat, we provide evidence-based maps predicting the possible locations across Africa where *An. stephensi* could establish if allowed to spread unchecked. Unsurprisingly, due to this species' close association with man-made habitats, our maps predict a high probability of presence within many urban cities across Africa where our estimates suggest that over 126 million people reside. Our results strongly support the WHO's call for surveillance and targeted vector control and provide a basis for the prioritization of surveillance.

vector | urban malaria | ensemble modeling | species distribution model | invasive species

Sub-Saharan Africa suffers the highest global levels of malaria mortality and morbidity (1). This is a direct consequence of the highly efficient mosquito vector species found on the continent, which include *Anopheles gambiae* ("the most dangerous animal in the world"), *Anopheles coluzzii*, *Anopheles funestus*, and *Anopheles arabiensis* (2–5). These dominant vector species have evolved alongside humans, becoming increasingly specialized in seeking out and feeding on human blood (2, 6).

Malaria has historically been considered to be a disease confined to rural locations (7). Ongoing urbanization and immigration into urban centers have resulted in cities with extensive areas of urban agriculture, untended green space, and unplanned urban sprawl with poor water management. Such areas share characteristics with rural sites and, consequently, mosquito vectors including both *An. arabiensis* and *An. gambiae* are able to maintain malaria transmission (7), in some cases, at prevalence rates up to 30 to 40% (8).

In contrast to the endemic African mosquitoes, the Asian malaria vector *Anopheles stephensi* is one of the few anopheline species found in central urban locations. This is presumed to be as a direct consequence of its ability to locate clean water in water storage tanks to lay its eggs (9). The more transient larval sites, such as puddles or ditches more commonly used by dominant African species, are more likely to be turbid or polluted (e.g., with oil or sewage) in urban settings and repel pollution-sensitive anophelines. However, there is increasing evidence that some African species are increasing their tolerance for "dirty" water. Sinka et al. (5) summarized the bionomics of the dominant

vector species in the published literature and found an equal number of studies (5:5) reported *An. arabiensis* in polluted, turbid water as were found in clear, clean habitats, with a similar result for *An. gambiae* (4:4). Nonetheless, urban *Plasmodium falciparum* transmission rates are repeatedly reported as significantly lower than those in peri-urban or rural areas (7, 10). Hay et al. (10) conducted a meta-analysis in cities from 22 African countries and reported a mean urban annual *P. falciparum* entomological inoculation rate [(APfEIR) of = 18.8] notably lower than the peri-urban (APfEIR = 63.9) or rural (APfEIR = 111.4 to 141.1) areas and concluded: "...there is clear evidence that urbanization affects anopheline species in the environment—diversity, numbers, survival rates, infection rates with *P. falciparum*, and the frequency with which they bite people are all affected."

*An. (Cellia) stephensi* (Liston) is capable of transmitting both *P. falciparum* and *Plasmodium vivax* parasites (9). It is a pervasive mosquito, with an extensive geographical range reaching from Thailand through the Indian Subcontinent, westward across the Arabian Peninsula and northward across southern China (9). Of the three known forms ("type", "intermediate", and "mysorensis") the type and intermediate forms of *An. stephensi* are efficient

## Significance

In 2012, an unusual outbreak of malaria occurred in Djibouti City followed by increasingly severe annual outbreaks. Investigations revealed the presence of an Asian mosquito species; *Anopheles stephensi*, which thrives in urban environments. *An. stephensi* has since been identified in Ethiopia and Sudan. By combining data for *An. stephensi* across its full range (Asia, Arabian Peninsula, Horn of Africa) with spatial models that identify the species' preferred habitat, we provide evidence-based maps predicting the possible African locations where *An. stephensi* could establish if allowed to spread. Our results suggest over 126 million people in cities across Africa could be at risk. This supports the WHO's call for targeted *An. stephensi* control and prioritized surveillance.

Author contributions: M.E.S. conceived the research; M.E.S. designed the research; M.E.S. performed the research; S.P. contributed primary modelling; N.C.M. updated the South-East Asian vector occurrence database to include all sibling species and data up to 2016; J.L. provided the background data points used in the model; C.L.M. conceived and created the PAR table; J.H., C.L.M., and K.J.W. provided technical advice; and M.E.S. wrote the paper with assistance from all authors.

The authors declare no competing interest.

This article is a PNAS Direct Submission.

This open access article is distributed under Creative Commons Attribution-NonCommercial-NoDerivatives License 4.0 (CC BY-NC-ND).

<sup>1</sup>To whom correspondence may be addressed. Email: marianne.sinka@zoo.ox.ac.uk or janet.hemingway@lstm.ac.uk.

<sup>2</sup>C.L.M. and K.J.W. contributed equally to this work.

This article contains supporting information online at <https://www.pnas.org/lookup/suppl/doi:10.1073/pnas.2003976117/-DCSupplemental>.

First published September 14, 2020.

vectors in both rural and urban environments (11–13), but it is its capacity to survive and proliferate in urban locations that separates this species from most of the other dominant vectors of malaria (9).

There is increasing evidence that this species is expanding its geographical range, with the type form being found for the first time in Sri Lanka in 2016 (14–16) and crossing from the Arabian Peninsula into Africa where it has been reported in Djibouti City in 2012, in Ethiopia in 2016 and 2018 [where it has now been described as “...widely distributed and established in Eastern Ethiopia” (17)] and Sudan (18–20).

Phylogenetic analyses of Ethiopian (Kebri Dehar) and Djibouti specimens reveal that these two populations are from different clades that originate from different sources in Pakistan (19). Despite only recently being detected, it is unknown how long *An. stephensi* may have actually been present in the Horn of Africa. Either it has spread very quickly, or it has remained unnoticed, possibly as a consequence of its preference to feed during twilight hours outdoors (assuming these characteristic behaviors reported from Asian *An. stephensi* are also found in African populations), allowing it to avoid capture using typical African mosquito survey methods. Indeed, Balkew et al. (17) comment that they captured few *An. stephensi* in their Centers for Disease Control and Prevention (CDC) light traps, and this is a method of survey often applied in Ethiopia. However, expert entomologists have surveyed widely in the Horn of Africa over many decades and, despite its known morphological resemblance to *An. arabiensis*, had *An. stephensi* been present, it would have been identified.

The incursion of *An. stephensi* into Africa is particularly worrying; over 40% of sub-Saharan Africans live in urban environments (21), prompting the World Health Organization (WHO) to issue a vector alert. They consider the presence of *An. stephensi* to be “...a major threat to malaria control and elimination in Africa...” (22), putting urban populations at significantly increased and potentially new risk of malaria transmission.

### The Increasing Range

Nearly a decade ago, a 4-y project collated georeferenced locational data for 41 dominant vector species of malaria, including *An. stephensi*. It resulted in the publication of a set of evidence-based species distribution maps derived from models identifying the environmental drivers that described the niche of each species (5, 9, 23). The maps predicted the probability of where, within its given range, each species was likely to be found.

The modeling methodology combined environmental covariates and occurrence data with an expert opinion (EO) species range, used to provide a boundary to the species' distributions. These EO polygons encompassed all of the known presence data and were agreed to be representative of the species' accepted range by an international group of vector experts. The EO ranges for the Asian-Pacific species were created in 2011 and were developed from the expert opinion range presented by White (24) in 1989.

As part of an ongoing study (25), we have updated our vector database of occurrences for the 19 species/species complexes of the Asian-Pacific region. It now includes presence data reported between 1985 to 2016 and has significantly increased the number of geolocated sites for *An. stephensi* from 251 to 358 confirmed locations.

To assess how far *An. stephensi* has expanded its range over the past decade, we overlaid the updated *An. stephensi* occurrence data, including points from Africa and Sri Lanka, on the 2011 EO range. The resulting map (Fig. 1) illustrates the new reports of *An. stephensi* across the Arabian peninsula and into the Horn of Africa. It starkly highlights the need for a contemporary assessment of this species' range.

### A Map of Environmental Suitability

Using the updated *An. stephensi* occurrence data, a set of background data (see methods), and *biomod2* [a species distribution modeling platform run using the R Project statistical software (26–29)], we created ensemble map projections of *An. stephensi* across its range and into Africa. The *biomod2* package allows comparison between multiple species distribution models; those performing well are then combined to create the final ensemble map, thus addressing uncertainties inherent in individual model methodologies. Our maps are composed of outputs from 500 model runs, using five species distribution modeling algorithms [Maximum Entropy (MAXENT) (30, 31), random forest (32), generalized boosted models (33), generalized additive models (34), and multiple adaptive regression splines (MARS) (35)].

Most species distribution models assume some level of equilibrium between the species and its environment (36, 37) whereas species that are invading and expanding into new locations are not stable. An ensemble model methodology will mitigate this instability to some extent (36, 38, 39), but it is important to note that our outputs include some extrapolation and we are predicting a species not yet at equilibrium.

To establish whether 1) the invading African *An. stephensi* is occupying a similar ecological niche to its Asian counterparts (i.e., is the invasion a consequence of a behavioral or ecological divergence), and 2) our models are accurately predicting suitable habitats in this new continent, we created two separate maps of habitat suitability in Africa: the first, our exclusive map, used all occurrence data except those from Africa and used the environmental associations found in Asia to predict habitat suitability in Africa. The second map, our inclusive projection, used the full occurrence database including those data from Africa.

We predict across the continent to highlight the potential environments this species could occupy if no action is taken. We discuss the maps in the context of the potential increased populations at risk (PAR) this expansion could cause as well as the likelihood of this “worst case scenario.”

### Results

Our map without African data (the exclusive map) used 343 occurrences. In comparison, the inclusive map used all 358 occurrences. Both models were provided with a set of seven environmental covariates, chosen as relevant to the ecology and bionomics of the dominant vectors of the Asian-Pacific region (*SI Appendix, Tables S1 and S2*). Both the inclusive and exclusive ensemble models selected the annual mean temperature to be most influential (*SI Appendix, Table S1*), with 86% of the models of the exclusive ensemble and 77.3% of the inclusive models selecting this as the primary influencing covariate. Human population density appears to be more important when the models include the African data, with 23.2% of the inclusive models selecting this variable first compared to 13.2% of the exclusive models. Temperature and human population density were most consistently selected either first or second in both the inclusive and exclusive models, and therefore of the covariates provided, are predicted to have the greatest influence on the niche of *An. stephensi*. Our evaluation statistics indicate the ensemble model is marginally better at predicting species distribution when the African data are included (Inclusive ensemble TSS: 0.907, ROC: 0.987; Exclusive ensemble: TSS: 0.897, ROC: 0.985).

To assess how the explanatory variables may influence the model outputs, response curves were generated for both the inclusive and exclusive models for all seven covariates (*SI Appendix, Fig. S2*). Mean annual temperature produced an expected unimodal response for both models, although the few additional African data appear to cause the model to predict a slightly increased optimal temperature range. The mean temperature calculated across all *An. stephensi* sites showed a slight increase when the 15 African

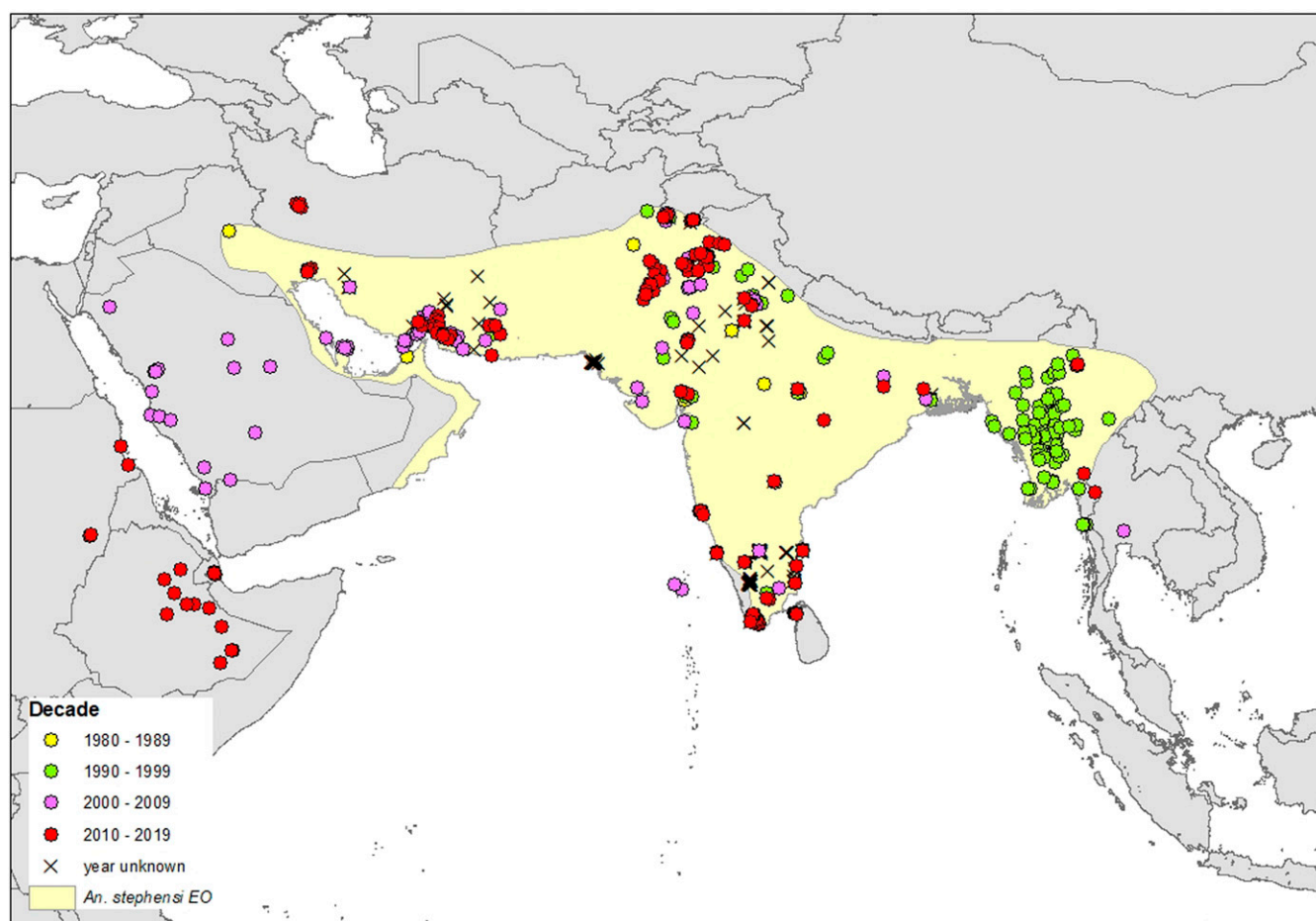


**Fig. 1.** The new “out of range” occurrence of *An. stephensi* in the Arabian Peninsula and Horn of Africa showing the 358 *An. stephensi* site locations used in our final species distribution models (SDMs) color coded by the decade in which they were sampled. The yellow shaded area shows the 2011 expert opinion range based on data published up to 31 October 2009 (9). Data showing the presence of *An. stephensi* more westerly across the Arabian peninsula (sampled in 2005 to 2006) were published after 2010. Thus *An. stephensi* may have been present but unreported or been expanding its range into western areas of the Arabian peninsula over the last 30 y.

sites were included (without African sites,  $x = 25.77^\circ\text{C}$ ,  $n = 343$ ), (with African sites,  $x = 25.94^\circ\text{C}$ ,  $n = 358$ ). The population density curve suggests an almost binary response; the presence of people equates to the presence of *An. stephensi*; however, mosquito vector surveys are unlikely to be conducted at uninhabited locations.

Overlaying the confirmed occurrence points in Africa over the exclusive ensemble map (Fig. 2) strongly suggests that the recent western expansion of *An. stephensi*, specifically inland from the established coastal populations, is due to some behavioral or niche adaptation. The model predicts the confirmed *An. stephensi* sites in Djibouti and in Semera and Jigjiga in Ethiopia well, with high predicted suitability, but fails to predict high suitability in Degehabur, Kebridehar, or Godey in Ethiopia. Coastal locations in Sudan are predicted as highly suitable, but inland sites are not.

### Populations at Risk (PAR)

Our final inclusive ensemble model was created using the full dataset, including those occurrences in Djibouti, Ethiopia, and Sudan. The inclusive map (Fig. 3), when compared to the exclusive output (Fig. 2), predicts all of the confirmed locations in Africa, including the inland sites in Ethiopia and Sudan. It demonstrates an increased area of predicted suitable habitat as a consequence of the wider range of conditions at locations where African *An. stephensi* have been found. Most of the locations

predicted to be highly suitable are urban, densely populated cities that traditionally incur low levels of malaria transmission. Many of these areas are, however, within malaria endemic zones, i.e., the surrounding rural and peri-urban locations have a parasite reservoir present within the local human populations and provide suitable habitats for the efficient dominant vector species primarily responsible for sub-Saharan Africa’s high malaria burden. The city environment currently provides a barrier to, or reduction in, malaria transmission but this would be removed when or if *An. stephensi* were able to establish. These densely populated areas may hold a significant reservoir of epidemiologically naïve people at high risk of malaria (depending on the level of population movement).

Using the Brinkoff City Population database (40), filtered to include only those cities with a population equal to or greater than one million, we overlaid the city locations on the inclusive ensemble map (Fig. 3 and *SI Appendix*, Fig. S2). The malaria endemic areas of Africa are shown in more detail in Fig. 4, which illustrates the predicted urban preference by *An. stephensi* in Africa. All African cities with one million inhabitants or more were assessed using the habitat suitability probability values generated by this study, their distance from the current records of *An. stephensi* collated by this study, and their distance from the malaria endemic zone. Table 1 is an abridged table, showing the top 15 cities, ordered by the increasing distance from the nearest



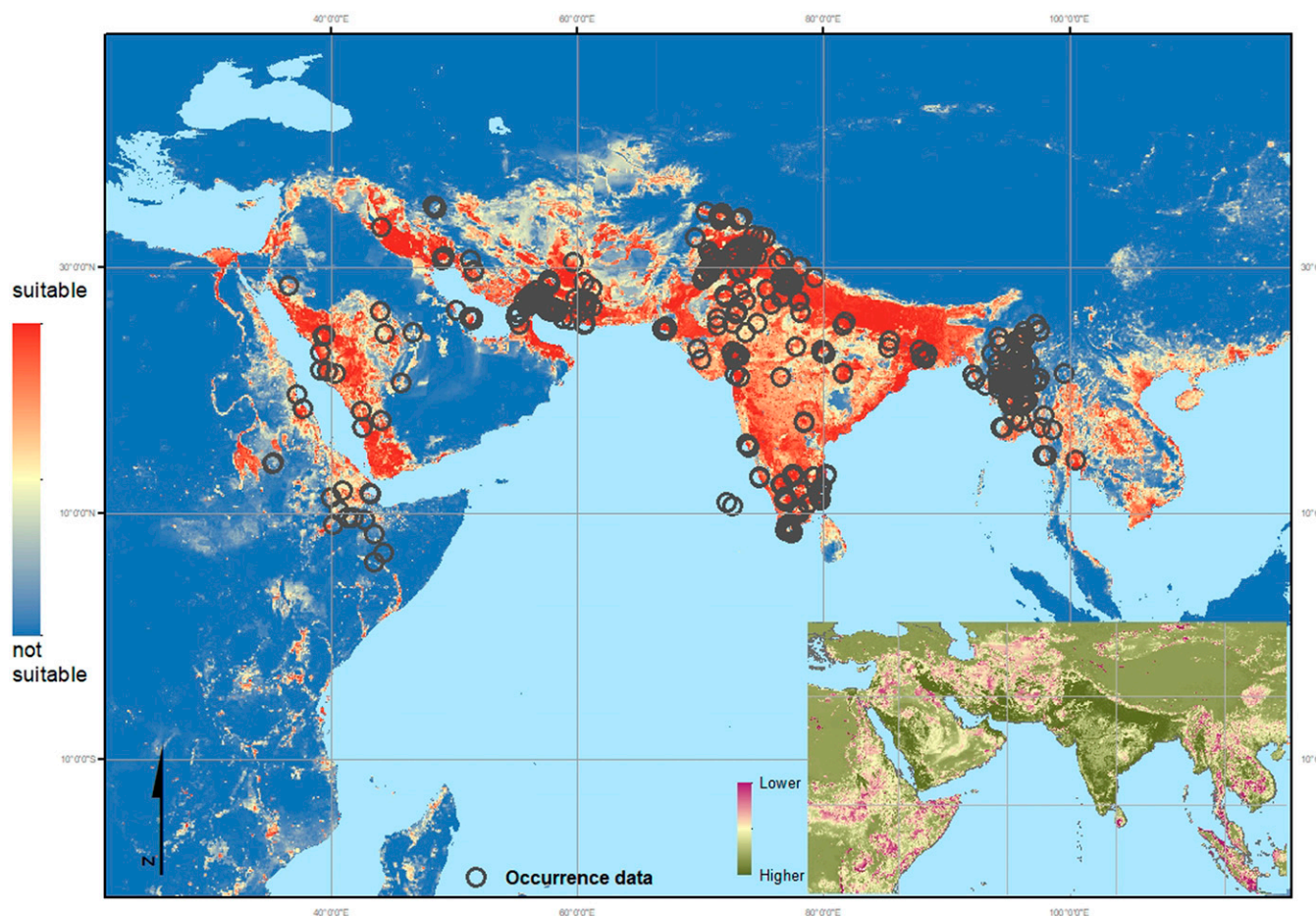


**Fig. 2.** Exclusive map: Environmental suitability map of *An. stephensi* using the updated occurrence database but without African sites. Red indicates a higher probability of environmental suitability whereas the blue indicates environments with a lower probability, i.e., more likely to be unsuitable for the species to occur. The environmental variables selected by the model as relevant to *An. stephensi* habitat suitability, in descending order (based on correlation score): Ann. Mean Temp. = 0.459, Human Pop<sup>n</sup> Dens. = 0.325, Precip (season) = 0.171, enhanced vegetation index (EVI) = 0.161, Irrigation = 0.155, tasselled cap wetness (TCW) = 0.110, Crop mosaic = 0.011. Dark gray circles indicate the location of all 358 occurrence data used in the final inclusive map (Fig. 3) including those in Africa (not used in this exclusive model). The thumbnail map shows the coefficient of variation calculated per pixel across the predicted range, indicating where the ensemble model provides the most reliable (higher confidence: dark green) and least reliable (lower confidence: red) predictions.

African site where *An. stephensi* has been confirmed as present (Djibouti, Ethiopia, or Sudan) that vary according to the predicted probability of *An. stephensi* establishing populations. The full table, listing 68 cities, is shown in the [SI Appendix, Table S3](#). The median and quartile values for the suitability predictions shown in Figs. 3 and 4, within the current extent of this species, were used to classify the habitat suitability within each city. Most (44/68) are predicted as highly suitable locations for *An. stephensi*. Of these 44 highly suitable cities, 36 are found within the current malaria endemic zone (Fig. 4 and [SI Appendix, Table S3](#)). As such, there could be an estimated additional 126 million people at risk for malaria if *An. stephensi* is able to continue its invasion across the continent.

### Bionomics

*An. stephensi* is a common laboratory species (as a consequence of its ability to breed in small containers), yet there are little quantified data describing the bionomics of *An. stephensi* in the wild. No reported entomological inoculation rate (EIR—the number of infected mosquito bites received per unit time) and only a single human biting rate value (HBR—the number of mosquito bites per unit time) could be found in the literature (42). In a brief summary of Asian species bionomics, Sinka et al. (9) indicate *An. stephensi* primarily prefers to feed on animals

(zoophilic) with examples of human biting (anthropophagy) indoors (endophagic) with outdoor (endophilic) resting behavior, but with examples of outdoor biting (exophagic) behavior, with a preference for biting during dusk (crepuscular) and the night. Similar to many of the Asian dominant vector species, *An. stephensi* appears to have some level of plasticity in its behavior, specifically in host choice, with rural *An. stephensi* tending to be more zoophilic than urban populations (42, 43). The mosquito's biting behavior is driven by host availability including human activity patterns and livestock sheltering practices. Fed female mosquitoes are reported as preferring to rest in poorly constructed buildings or animal sheds (42–45). Such structures are characteristic of unplanned urban sites and can be found around and within many rapidly expanding cities in Africa (46, 47).

Many malaria vector surveys include hourly mosquito catches that run between 6 PM and 6 AM, when anopheline vectors are typically most active. Using data from the Malaria Atlas Project's bionomics database (48), nightly activity for the three primary African vector species (*An. gambiae*, *An. arabiensis*, and *An. funestus*) are compared with *An. stephensi* (Fig. 5). This simple plot illustrates that *An. stephensi* has peak activity (i.e., is actively seeking a blood meal) earlier in the evening than any of the African dominant vector species (DVS) with over half of the total bites from this species occurring within the first quarter of

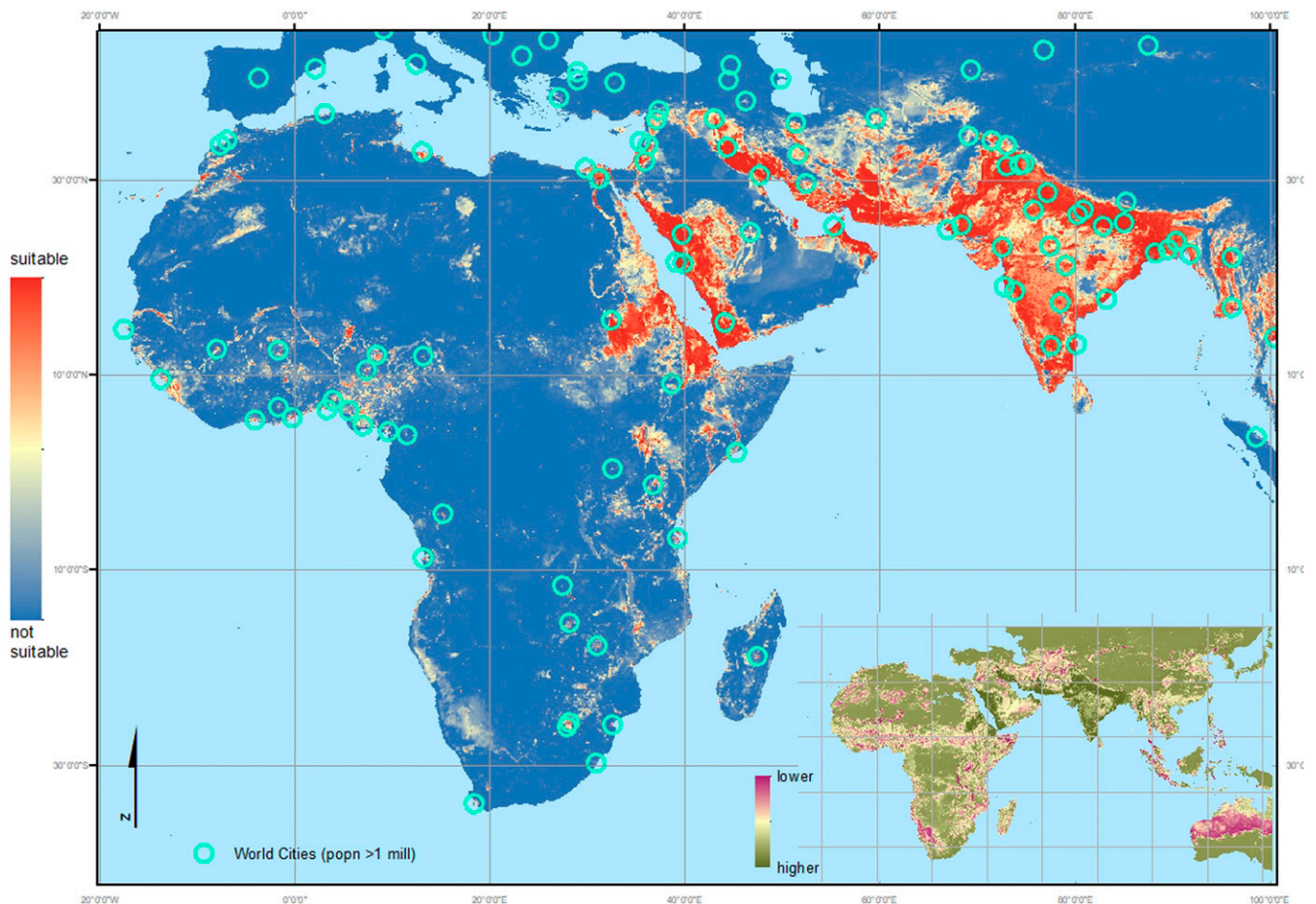


**Fig. 3.** Inclusive map: Environmental suitability map of *An. stephensi* using the updated occurrence database including all African sites. Red indicates a higher probability of environmental suitability whereas the blue indicates environments with a lower probability, i.e., more likely to be unsuitable for the species to occur. The environmental variables selected by the model as relevant to *An. stephensi* habitat suitability, in descending order (based on correlation score): Ann. Mean Temp. = 0.461, Human Pop<sup>n</sup> Dens. = 0.370, EVI = 0.174, Precip (season) = 0.161, TCW = 0.134, Irrigation = 0.130, Crop mosaic = 0.010. Turquoise circles indicate the location of cities with a population > 1 million. The thumbnail map shows the coefficient of variation calculated per pixel across the predicted range, indicating where the ensemble model provides the most reliable (higher confidence: dark green) and least reliable (lower confidence: red) predictions.

the night (6 PM to 9 PM). Activity can be observed later, but at a much lower rate (42). African vector species are known to prefer to bite when humans are asleep and vulnerable, and as expected, *An. gambiae* and *An. funestus* both have peak activity well into the night (third quarter: midnight to 3 AM). Whether newly establishing African *An. stephensi* populations maintain a preference for biting in the evening remains to be seen, and there is some indication that it may change its outdoor biting activity depending on the season (42). However, its crepuscular biting preference would allow *An. stephensi* to bypass insecticide treated bednets; the most widely used (and currently most effective) mosquito interventions used across Africa (49, 50). *An. stephensi* larvae have been found coexisting in water storage containers with *Aedes aegypti* (a vector of yellow fever and dengue among others) and *Culex quinquefasciatus* (the southern house mosquito—vector of lymphatic filariasis and West Nile fever) so interventions already in place to target these mosquitoes, as well as better management of urban infrastructure including water and green spaces, could help control *An. stephensi* (51–53).

*An. stephensi* is known to have a seasonal peak in abundance, normally in the late spring/early summer months (42, 43, 54), and shows some regulation by climatic conditions; here we have seen annual temperature is the most influential covariate in describing this species' niche. In urban areas, *An. stephensi* has been found

in roof gutters, domestic wells, air conditioning units, and cisterns (9, 52, 55). It is not reliant on rainfall to fill its larval sites like many other species (e.g., *An. gambiae* that makes use of temporary rain-filled puddles), but takes advantage of human built and maintained water storage facilities, particularly cement or brick structures (19, 20, 42, 43, 52, 55, 56); a necessity to the human urban populations during the dry summer months. Indeed, it is *An. stephensi*'s ability to utilize such human built water storage tanks that may have facilitated its ability to expand its range (15). Within our model, human population density was also a highly influential variable and our final ensemble map suggests that many large urban expanses are highly suitable if this species continues to invade Africa, whereas most rural areas are not.

## Discussion

*An. stephensi* is evidently expanding its geographic range (Fig. 1). Whether this is a recent event or has occurred over the longer term is still unclear. Nonetheless, this invasion has already been implicated in recent outbreaks of urban malaria in Djibouti (20). Djibouti was entering the pre-elimination stage, with the last outbreak of malaria reported in 1999. However, in January 2013, outbreaks of *P. falciparum* were reported, predominantly in Djibouti City, including historically malaria-free locations that were considered to lack suitable anopheline larval habitats (20).



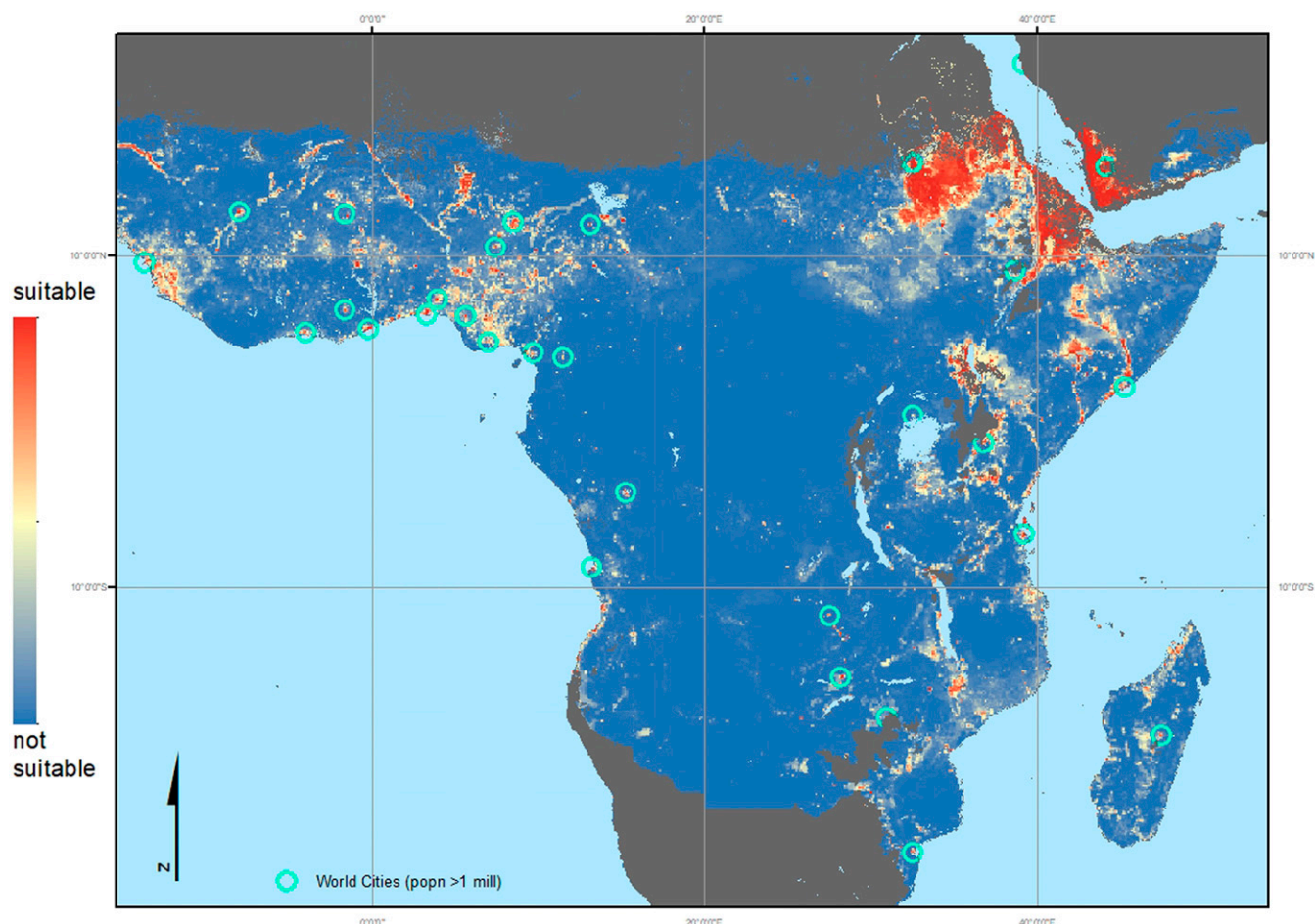


**Fig. 4.** The inclusive map focusing on the malaria (*P. falciparum* and *P. vivax* [PfPr]) endemic areas in Africa: Environmental suitability map of *An. stephensi* using the updated occurrence database including all African sites, masked (dark gray) using the Malaria Atlas Project (MAP) PfPr endemicity mask (16). Red indicates a higher probability of environmental suitability whereas the blue indicates environments with a lower probability, i.e., more likely to be unsuitable for the species to occur. Turquoise circles indicate the location of cities with a population > 1 million.

Since 2013, outbreaks have recurred annually in the city with increasing intensity. Reported and confirmed cases in the country have increased from only 25 in 2012 to 9,473 in 2015 (57) and 14,810 cases reported in 2017 (18). *An. stephensi* is highly susceptible to infection by African *P. falciparum* isolates (58) and also *P. vivax*. Vivax transmission was reported in Djibouti for the first time in 2016, and again in 2017 (18). Further, there is some indication that *An. stephensi* may already be adapting to the African environment, changing from predominantly seasonal activity reported between 2013 to 2016 to year-round activity from 2017 (18).

Carter et al. (19) provide genetic evidence that the Djibouti and Ethiopian *An. stephensi* populations are a result of separate introduction events, both originating from Pakistan. Our exclusive model was able to predict the Djibouti populations but not the full extent of the Ethiopian sites, indicating some variation in the niche characteristics between the Djibouti and Ethiopian populations. Whether these adaptations are intrinsic in the original Pakistan populations (suggesting the full extent of the Asian niche has yet to be described) or have occurred since its expansion into Africa, can only be teased apart with further phylogenetic analyses. However, when comparing the exclusive and inclusive ensemble maps over Asia, there appears to be very little difference in the predicted extent, suggesting these additional data are not adding new niche information to the predictions in Asia.

It is likely that *An. stephensi* individuals have been inadvertently introduced into Africa on multiple occasions, but it appears that,

in Djibouti at least, this species has only recently established persistent populations. The situation in Ethiopia remains less clear; Balkew et al. (17) report *An. stephensi* as widespread across eastern Ethiopia and hypothesize that either *An. stephensi* is a recent introduction or that it has been present but remained undetected due to morphological similarity to *An. arabiensis*. Whether the specimens from Sudan clarify the situation or raise further questions is yet to be seen.

Species distribution models provide a snapshot of the species' suitable niche based on a set of criteria defined by the covariates provided to the model at the locations where the species has been shown to be present. This correlative approach does not, however, provide a mechanistic interpretation of how the species came to exist within that niche and the predicted output does not always consider biological and physical barriers to species movement.

Our database is the most comprehensive set of dated and geolocated, species-specific occurrence records currently available. However, as with all presence data, it provides information about a single point in space and time; although we know the date of sampling, we do not know how long prior to that positive occurrence *An. stephensi* has been inhabiting that site, nor if it continues to exist there. These records can be considered opportunistic sampling and do not come from continuous monitoring programs. They do not fully represent the geographical and environmental space considered by our study. Thus we cannot use this

**Table 1. Abridged table showing the populations at risk if *An. stephensi* were to establish in urban cities of Africa (full table in [SI Appendix](#))\***

City	Country	Population	Distance from <i>A. stephensi</i> records (km)	Distance from malaria endemic zone (km)	Habitat suitability class
Djibouti City	Djibouti	<1 M	0	0	1
Addis Ababa	Ethiopia	3,725,000	160	0*	2
Asmara	Eritrea	<1 M	450	0	1
Muqdisho (Mogadishu)	Somalia	1,890,000	480	0	1
Al-Khartum (Khartoum)	Sudan	6,150,000	940	0	1
Nairobi	Kenya	5,950,000	1,100	0	1
Mombasa	Kenya	1,240,000	1,190	0	1
Kampala	Uganda	3,400,000	1,280	0	2
Dar es Salaam	Tanzania	6,150,000	1,490	0	1
Kigali	Rwanda	1,140,000	1,650	0	2
Kisangani	DRC	1,120,000	1,900	0	3
Al-Qahirah (Cairo)	Egypt	20,500,000	2,260	1,490	1
Bangui	CAR	1,160,000	2,440	0	2
Lilongwe	Malawi	1,020,000	2,450	0	1
Mbuji-Mayi	DRC	2,000,000	2,490	0	2

The cities are listed in order of increasing distance from confirmed *An. stephensi* presences in Africa and many of the cities that are not shown in the abridged version are identified as highly suitable ([SI Appendix, Table S3](#)). The habitat suitability for *An. stephensi* classification was evaluated from the predicted habitat suitability map (Fig. 3). The quartiles for the full distribution of predicted values within the current species range were calculated and used to assign suitability class. Class 4 (below the lower quartile, indicating lowest suitability) is not found in any listed city (full table in [SI Appendix, Table S3](#)). Classes 3 (indicated as pale blue) and 2 (pale yellow) indicate increasing increments of suitability, with class 1 (red) indicating the highest suitability (i.e., predictions greater than the upper quartile value). Population data are taken from Brinkoff (40) listing urban agglomerations with  $\geq 1$  million inhabitants. The distance from *An. stephensi* records (data collated by this study) was calculated in QGIS (41) using United Nations (UN) sourced city coordinates which were also used to evaluate the distance from *P. falciparum* and *P. vivax* endemic zones (16). The 11 cities closest to the current *An. stephensi* distribution are all within the malaria endemic zone.

\*Addis Ababa is within the area of the malaria endemic zone, but due to its altitude (~2300 m) is considered nonendemic.

modeling technique to help answer questions about how and why *An. stephensi* appears to be expanding its range.

Nonetheless, generating response curves provides some indication of the potential niche width and how *An. stephensi* interacts with specific environmental covariates supplied to the model. Here, as expected, we see a unimodal response to temperature, suggesting that there are sites represented that are beyond the optimal temperature for the species to exist. Moreover, we see that the few additional sites in Africa appear to expand the optimal temperature range, which could suggest a recent potential expansion of its thermal niche (although as this is based on few data, it should be treated with caution).

A recent study that modeled the environmental suitability of malaria transmission and temperature using *An. stephensi* data compared to multispecies models (primarily using *An. gambiae*

data), reported a wider thermal niche in the *An. stephensi* model (59). It implicated *An. stephensi* as having a thermal minimum 3.4 °C lower and thermal maximum 3.4 °C higher than the multispecies estimates. *An. stephensi* is active at dusk and as such may have more tolerance for higher temperatures than typical anophelines that tend to become active later in the evening. Moreover, as an urban species, *An. stephensi* are routinely exposed to higher temperatures generated within cities (the urban heat island effect) compared to rural counterparts and could be more buffered from the influence of climate than rural species.

Increasing or changing climatic temperature does not appear to explain the movement of this mosquito across the Arabian peninsula and into Africa. It is more likely to be due to the movement of people and livestock. Indeed, presences reported from Ethiopia appear to be located along primary transportations

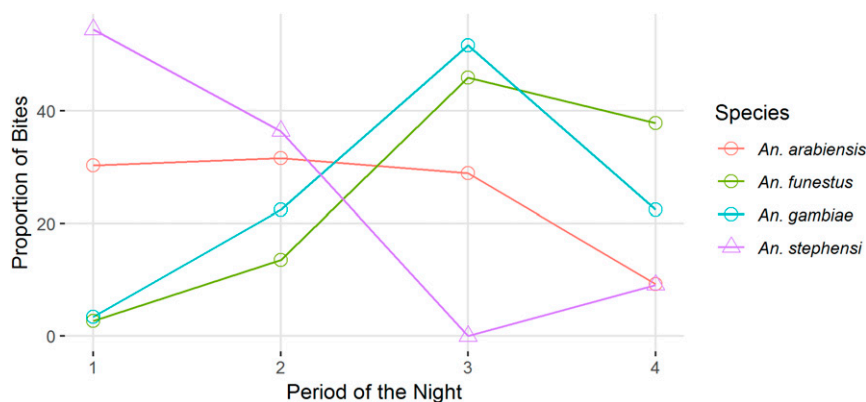


**Fig. 5. Mosquito biting activity summarized from published studies (MAP bionomics database) comparing the Asian (open triangles) *An. stephensi* with the African (open circles) DVS (*An. arabiensis*, *An. gambiae*, and *An. funestus*) showing the peak activity periods as the proportion of mosquitoes biting in the first, second, third and fourth quarters of the night (from 6 PM to 6 AM).**

routes, although a full randomized survey would be needed to confirm these observations. With African cities growing at an extraordinary rate and 43% of Africans now living in urban areas (60), the movement of people into urban sites and the observation that *An. stephensi* is spreading via key transportation routes, mean it is not inconceivable that this species could be transported large distances and that this may not remain a problem centered on the Horn of Africa. As illustrated in Fig. 3, many cities across the whole of Africa contain potentially suitable habitats for *An. stephensi*. For example, due to its high population density, Nigeria, appears to be particularly suitable.

The escalation of urban Falciparum malaria, as well as emerging Vivax in Djibouti (18, 20), needs to act as a stark warning, one succinctly summarized by Takken and Lindsay (61): “If... [*An. stephensi*] invades large cities, such as Khartoum, Sudan; Mombasa, Kenya; and Dar es Salaam, the region could face malaria outbreaks of unprecedented size.” Once established, *An. stephensi* is difficult to control. Traditional mosquito interventions via indoor residual spraying and treated bednets are notably more difficult to implement in cities, and the crepuscular biting habits of *An. stephensi* suggest they may have less impact on this species than the dominant African vectors.

*An. stephensi* is not the first malaria vector to invade a new continent. In one notable historic example, a member of the *An. gambiae* complex [since shown to be *An. arabiensis* (62)] established in the city of Natal, north-eastern Brazil. Similar to the current situation, the presence of *An. arabiensis* was accompanied by a significant increase in malaria transmission (63). Although *An. arabiensis* was quickly eliminated from the city, the larval treatment used was not extended to the surrounding areas and thus *An. arabiensis* was able to move out of the city unnoticed (dubbed the “silent spread”) and increase its population until eventually a “catastrophic malaria epidemic” (64) began in 1938 within the states of Rio Grande do Norte and Ceará (63, 64). It took the formation of a new anti-malaria service and a multimillion dollar budget to finally eradicate this mosquito from Brazil (64). This is a lesson in history that would be advisable to note when considering the future course of action against *An. stephensi* in Africa.

The recent reports of *An. stephensi* in Africa combined with our ensemble maps presented here highlight a substantial future threat to urban African populations (65). The WHO are urging member states in and around the Horn of Africa, the Republic of the Sudan, and surrounding geographical areas to take immediate action including active vector surveillance and reporting, assessing the ecological characteristics if the mosquito is found, as well as assessing insecticide resistance (22). Here our inclusive map provides an evidence-based indication of where the environmental conditions may be suitable for *An. stephensi* to thrive. We distinguish cities that are predicted to be highly suitable within the current malaria endemic zone and those outside it. For example, in the case of cities such as Cairo that are distant from malaria endemic regions in Africa and the Middle East, the

potential threat will only become a reality if both the vector and the parasite are introduced (66).

Targeted surveillance is now needed to monitor the existing populations in Africa, optimize the strategies for its control, and ensure that this species does not continue its invasion across Africa.

## Conclusion

Using a comprehensive and updated dataset incorporating the recently identified occurrence sites in Africa, our predictive map provides an evidence-base for the possible expansion of *An. stephensi* across Africa and, as expected, the probability of occurrence is much higher in the more densely populated areas where huge numbers of people could be at risk. We predict an increased PAR of up to 126 million people if *An. stephensi* were to occupy this predicted niche. If it continues its incursion into the African continent unchecked, there is a very real possibility of mass outbreaks of malaria among naïve populations in areas of vector-parasite coexistence. In a continent striving to improve and strengthen its health systems, such a huge burden could be catastrophic. Targeted vector surveillance is therefore urgently needed.

## Materials and Methods

Our maps were created using an updated database of *An. stephensi* occurrence ranging from 1985 to 2019, including those sites reported from the Horn of Africa (SI Appendix). Our background dataset included presences for anopheline species (excluding *An. stephensi*), *Aedes*, and *Culex* species across Asia and within the Horn of Africa. We provided a final set of seven relevant environmental covariates, refined from an initial set of 19, and run our models using the *biomed2* platform (28, 29) in R studio (version 1.2.1335) (27) using R (version 3.6.1) (26). This platform allows the comparison of multiple distribution model methodologies to provide a consensus map based on those evaluated [True Skill Statistic (TSS) and the area under the receiver operating curve (ROC)] to have the best predictive performance. We provide a Coefficient of Variation map alongside our consensus map. This is a simple evaluation that illustrates areas where the confidence in the model predictions are lower (i.e., where data are sparse). We also provide the ranked, model-selected influential variables, generated in *biomed2*, to show which covariates are having the highest influence within the model and the final consensus map.

To evaluate the potential effect of the spread of *An. stephensi*, we estimated the populations at risk for all cities with over one million inhabitants based on our predicted maximum suitability values from the pixels within the city. Using QGIS (41), the distance to locations confirmed as having *An. stephensi* were calculated as well as the distance from the combined *P. falciparum* and *P. vivax* endemic zone (16).

**Data Availability.** The full occurrence dataset used to generate our maps are available via Dryad [*An. stephensi* occurrence data 1985 to 2019, Dryad, Dataset, <https://doi.org/10.5061/dryad.3xsj3txcx> (67)].

**ACKNOWLEDGMENTS.** This work was funded by the Google Impact Challenge award (Mosquito Detection Project DFR01520 - HumBug) and Wellcome grant 108440/Z/15/Z. Additional thanks to Ian Ondo for mapping advice, Seth Irish, Dave Weetman and colleagues for providing additional data, Marybel Soto Gomez for assisting in running our final models, and to Dan Strickman for a query that inspired this work in the first place.

- World Health Organization, *World Malaria Report*, (World Health Organization, Geneva, 2018), p. 210.
- M. Coetzee, Distribution of the African malaria vectors of the *Anopheles gambiae* complex. *Am. J. Trop. Med. Hyg.* **70**, 103–104 (2004).
- M. Coluzzi, The clay feet of the malaria giant and its African roots: Hypotheses and inferences about origin, spread and control of *Plasmodium falciparum*. *Parassitologia* **41**, 277–283 (1999).
- M. T. Gillies, B. de Meillon, *The Anophelinae of Africa South of the Sahara (Ethiopian Zoogeographical Region)*, (The South African Institute for Medical Research, Johannesburg, ed. 2, 1968).
- M. E. Sinka et al., The dominant *Anopheles* vectors of human malaria in Africa, Europe and the Middle East: Occurrence data, distribution maps and bionomic précis. *Parasit. Vectors* **3**, 117 (2010).
- J. D. Charlwood et al., Density-independent feeding success of malaria vectors (Diptera: Culicidae) in Tanzania. *Bull. Entomol. Res.* **85**, 29–35 (1995).
- V. Robert et al., Malaria transmission in urban sub-Saharan Africa. *Am. J. Trop. Med. Hyg.* **68**, 169–176 (2003).
- H. J. Overgaard et al., Malaria transmission after five years of vector control on Bioko Island, Equatorial Guinea. *Parasit. Vectors* **5**, 253 (2012).
- M. E. Sinka et al., The dominant *Anopheles* vectors of human malaria in the Asia-Pacific region: Occurrence data, distribution maps and bionomic précis. *Parasit. Vectors* **4**, 89 (2011).
- S. I. Hay, C. A. Guerra, A. J. Tatem, P. M. Atkinson, R. W. Snow, Urbanization, malaria transmission and disease burden in Africa. *Nat. Rev. Microbiol.* **3**, 81–90 (2005).
- B. A. Rao, W. C. Sweet, A. M. Subba Rao, Ova measurements of *A. stephensi* type and *A. stephensi* var. *mysorensis*. *J. Malar. Inst. India* **1**, 261–266 (1938).
- S. K. Subbarao, K. Vasantha, T. Adak, V. P. Sharma, C. F. Curtis, Egg-float ridge number in *Anopheles stephensi*: Ecological variation and genetic analysis. *Med. Vet. Entomol.* **1**, 265–271 (1987).
- W. C. Sweet, B. A. Rao, Races of *A. Stephensi* liston, 1901. *Ind. Med. Gaz.* **72**, 665–674 (1937).
- S. N. Surendran et al., Genotype and biotype of invasive *Anopheles stephensi* in mannar Island of Sri Lanka. *Parasit. Vectors* **11**, 3 (2018).



15. S. N. Surendran *et al.*, Anthropogenic factors driving recent range expansion of the malaria vector *Anopheles stephensi*. *Front. Public Health* **7**, 53 (2019).
16. Malaria Atlas Project (MAP). <https://malariaatlas.org/>. Accessed 1 September 2020.
17. M. Balkew *et al.*, Geographical distribution of *Anopheles stephensi* in eastern Ethiopia. *Parasit. Vectors* **13**, 35 (2020).
18. M. Seyfarth, B. A. Khaireh, A. A. Abdi, S. M. Bouh, M. K. Faulde, Five years following first detection of *Anopheles stephensi* (Diptera: Culicidae) in Djibouti, Horn of Africa: Populations established-malaria emerging. *Parasitol. Res.* **118**, 725–732 (2019).
19. T. E. Carter *et al.*, First detection of *Anopheles stephensi* Liston, 1901 (Diptera: Culicidae) in Ethiopia using molecular and morphological approaches. *Acta Trop.* **188**, 180–186 (2018).
20. M. K. Faulde, L. M. Rueda, B. A. Khaireh, First record of the Asian malaria vector *Anopheles stephensi* and its possible role in the resurgence of malaria in Djibouti, Horn of Africa. *Acta Trop.* **139**, 39–43 (2014).
21. World Bank, <https://data.worldbank.org/indicator/SP.URB.TOTL.IN.ZS?locations=ZG>. Accessed 1 September 2020.
22. World Health Organization, Vector Alert: *Anopheles stephensi* invasion and spread. <https://www.who.int/news-room/detail/26-08-2019-vector-alert-anopheles-stephensi-invasion-and-spread>. Accessed 1 September 2020.
23. M. E. Sinka *et al.*, The dominant *Anopheles* vectors of human malaria in the Americas: Occurrence data, distribution maps and bionomic précis. *Parasit. Vectors* **3**, 72 (2010).
24. G. B. White, *Geographical Distribution of Arthropod-Borne Diseases and their Principal Vectors*, (World Health Organization, Division of Vector Biology and Control, Geneva, 1989), pp. 7–22.
25. HumBug, <http://humbug.ac.uk/>. Accessed 1 September 2020.
26. The R Foundation for Statistical Computing, *R: A Language and Environment for Statistical Computing, Version 3.6.1: "Action of the toes."* (The R Foundation for Statistical Computing, Vienna, Austria 2019).
27. RStudio Team, RStudio: Integrated Development for R. <http://www.rstudio.com>. Accessed 1 September 2020.
28. W. Thuiller, BIOMOD—Optimizing predictions of species distributions and projecting potential future shifts under global change. *Glob. Change Biol.* **9**, 1353–1362 (2003).
29. W. Thuiller, B. Lafourcade, R. Engler, M. B. Araujo, BIOMOD—A platform for ensemble forecasting of species distributions. *Ecography* **32**, 369–373 (2009).
30. S. J. Phillips, R. P. Anderson, R. E. Schapire, Maximum entropy modeling of species geographic distributions. *Ecol. Modell.* **190**, 231–259 (2006).
31. J. Elith *et al.*, A statistical explanation of MaxEnt for ecologists. *Divers. Distrib.* **17**, 43–57 (2011).
32. L. Breiman, Random forests. *Mach. Learn.* **45**, 5–32 (2001).
33. J. Elith, J. R. Leathwick, T. Hastie, A working guide to boosted regression trees. *J. Anim. Ecol.* **77**, 802–813 (2008).
34. T. J. Hastie, R. J. Tibshirani, *Generalized Additive Models*, (Chapman and Hall/CRC, 1990).
35. J. H. Friedman, Multivariate adaptive regression splines. *Ann. Stat.* **19**, 1–67 (1991).
36. J. Elith, M. Kearney, S. Phillips, The art of modelling range-shifting species. *Methods Ecol. Evol.* **1**, 330–342 (2010).
37. O. Broennimann, A. Guisan, Predicting current and future biological invasions: Both native and invaded ranges matter. *Biol. Lett.* **4**, 585–589 (2008).
38. R. Engler *et al.*, Combining ensemble modeling and remote sensing for mapping individual tree species at high spatial resolution. *For. Ecol. Manage.* **310**, 64–73 (2013).
39. M. Marmion, M. Parviainen, M. Luoto, R. K. Heikkinen, W. Thuiller, Evaluation of consensus methods in predictive species distribution modelling. *Divers. Distrib.* **15**, 59–69 (2009).
40. T. Brinkhoff, City population, <http://www.citypopulation.de/>. Accessed 1 September 2020.
41. QGIS, QGIS Geographic Information System. Open Source Geospatial Foundation Project. <https://qgis.org/en/site/>. Accessed 1 September 2020.
42. O. P. Singh, "Bionomics of malaria vectors in India." in *Vector Biology*, (Malaria Research Centre, 2002), pp. 19–31.
43. C. P. Batra, T. Adak, V. P. Sharma, P. K. Mittal, Impact of urbanization on bionomics of *An. culicifacies* and *An. stephensi* in Delhi. *Indian J. Malariol.* **38**, 61–75 (2001).
44. K. K. Chatterjee, D. Biswas, D. K. Choudhuri, H. Mukherjee, A. K. Hati, Resting sites of *Anopheles stephensi* liston in Calcutta. *Indian J. Malariol.* **30**, 109–112 (1993).
45. A. K. Hati, K. K. Chatterjee, D. Biswas, Daytime resting habits of *Anopheles stephensi* in an area of Calcutta. *Indian J. Malariol.* **24**, 85–87 (1987).
46. United Nations, African Renewal. <https://www.un.org/africarenewal/magazine/april-2012/towards-african-cities-without-slums>. Accessed 1 September 2020.
47. UNHABITAT, *The State of African Cities 2018—The geography of African Investment*, (Erasmus University Rotterdam (EUR): United Nations Human Settlements Programme (UN-Habitat), 2018).
48. N. C. Massey *et al.*, A global bionomic database for the dominant vectors of human malaria. *Sci. Data* **3**, 160014 (2016).
49. S. Bhatt *et al.*, The effect of malaria control on *Plasmodium falciparum* in Africa between 2000 and 2015. *Nature* **526**, 207–211 (2015).
50. G. F. Killeen *et al.*, Going beyond personal protection against mosquito bites to eliminate malaria transmission: Population suppression of malaria vectors that exploit both human and animal blood. *BMJ Glob. Health* **2**, e000198 (2017).
51. S. Chakraborty, S. Ray, N. Tandon, Seasonal prevalence of *Anopheles stephensi* larvae and existence of two forms of the species in an urban garden in Calcutta City. *Indian J. Malariol.* **35**, 8–14 (1998).
52. T. Mariappan, V. Thenmozhi, P. Udayakumar, V. Bhavaniamadevi, B. K. Tyagi, An observation on breeding behaviour of three different vector species (*Aedes aegypti* Linnaeus 1762, *Anopheles stephensi* Liston 1901 and *Culex quinquefasciatus* Say 1823) in wells in the coastal region of Ramanathapuram district, Tamil Nadu, India. *Int. J. Mosq. Res.* **2**, 42–44 (2015).
53. D. Weetman *et al.*, *Aedes* mosquitoes and *Aedes*-borne Arboviruses in Africa: Current and future threats. *Int. J. Environ. Res. Public Health* **15**, 220 (2018).
54. A. Mehravaran *et al.*, Ecology of *Anopheles stephensi* in a malarious area, southeast of Iran. *Acta Med. Iran.* **50**, 61–65 (2012).
55. D. Biswas, R. N. Dutta, S. K. Ghosh, K. K. Chatterjee, A. K. Hati, Breeding habits of *Anopheles stephensi* Liston in an area of Calcutta. *Indian J. Malariol.* **29**, 195–198 (1992).
56. R. S. Sharma, Urban malaria and its vectors *Anopheles stephensi* and *Anopheles culicifacies* (Diptera: Culicidae) in Gurgaon, India. *Southeast Asian J. Trop. Med. Public Health* **26**, 172–176 (1995).
57. World Health Organization, Djibouti country profile. <http://apps.who.int/gho/data/node.country.country-DJI>. Accessed 1 September 2020.
58. J. C. Hume, M. Tunnicliffe, L. C. Ranford-Cartwright, K. P. Day, Susceptibility of *Anopheles gambiae* and *Anopheles stephensi* to tropical isolates of *Plasmodium falciparum*. *Malar. J.* **6**, 139 (2007).
59. K. L. Miazgowski *et al.*, Mosquito species and age influence thermal performance of traits relevant to malaria transmission. *bioRxiv*:10.1101/769604 (14 September 2019).
60. United Nations DoEaSA, *Population Division: World Urbanization Prospects: The 2018 Revision*, (United Nations, New York, 2019).
61. W. Takken, S. Lindsay, Increased threat of urban malaria from *Anopheles stephensi* mosquitoes, Africa. *Emerg. Infect. Dis.* **25**, 1431–1433 (2019).
62. A. Parmakelis *et al.*, Historical analysis of a near disaster: *Anopheles gambiae* in Brazil. *Am. J. Trop. Med. Hyg.* **78**, 176–178 (2008).
63. G. Lopes, *Anopheles gambiae* in Brazil: The background to a "silent spread," 1930–1932. *Hist. Cienc. Saude Manguinhos* **26**, 823–839 (2019).
64. G. F. Killeen, U. Fillinger, I. Kiche, L. C. Gouagna, B. G. Knols, Eradication of *Anopheles gambiae* from Brazil: Lessons for malaria control in Africa? *Lancet Infect. Dis.* **2**, 618–627 (2002).
65. Q. Qi *et al.*, The effects of urbanization on global *Plasmodium vivax* malaria transmission. *Malar. J.* **11**, 403 (2012).
66. W. K. Reisen, Landscape epidemiology of vector-borne diseases. *Annu. Rev. Entomol.* **55**, 461–483 (2010).
67. M. E. Sinka *et al.*, *An. stephensi* occurrence data 1985 to 2019. Dryad. <https://doi.org/10.5061/dryad.3xsj3tccx>. Deposited 17 June 2020.